MAPPING OF [H_2O], [HDO], AND [HDO]/[H_2O] ON MARS USING GROUND BASED HIGH-RESOLUTION SPECTROSCOPY.

R.E. Novak , *Iona College, New Rochelle NY USA, (rnovak@iona.edu),* **M. J. Mumma, G. L. Villanueva,** NASA-*Goddard Space Flight Center, Greenbelt, MD, USA*

Introduction:

We report recent investigations of HDO and H_2O on Mars for data taken on 26 March 2008 (L_s = 50.1°) and 3 April 2010 (L_s = 72.5°). Our objective is to obtain measurements of the seasonal and latitudinal variation of the [HDO]/[H_2O] ratio and thereby obtain better insights into the dynamics of Mars' atmosphere. The preferential escape of the lighter hydrogen isotope controls the global [HDO]/[H_2O] abundance ratio. A comparison of the present abundance level with escape models provides an estimate of the amount of water lost over time. Furthermore, Mars water undergoes seasonal cycling and (perhaps) bulk fractionation in polar ice or even aerosols. Models [1] have showing that the [HDO]/[H_2O] ratio of atmospheric water vapor has both a seasonal and latitudinal variation. The recent discovery of methane on Mars [2,3,4] has led to much discussion on its origin and destruction [5,6]. The chemistry of methane production (whether biotic or abiotic) is closely linked to the presence of water. It is therefore important to establish the [HDO]/[H_2O] ratio in water released with methane on Mars.

Our group has conducted an observing program to measure the [HDO]/[H_2O] ratio. DiSanti and Mumma [7] developed a technique for mapping HDO on Mars through its ν_1 fundamental band near 3.67 μm using CSHELL at the NASA IRTF. Novak et al. [8] extended the approach significantly and describe nearly simultaneous measurements of ozone and HDO on Mars acquired in January 1997. For data taken from 1997 to 2003, we compared our HDO data to H_2O results obtained from TES [9]. Since 2003, we have been using absorption lines near 3.33 μm (the $2\nu_2$ band) to determine H_2O abundances. With long slit spectrometers, we now map the two species using the same spectrometer-telescope combination, eliminating many sources of systematic error.

We have reported our results and methods for obtaining and analyzing column densities of H_2O, HDO, and the corresponding [HDO]/[H_2O] ratio [8,10,11,12,12,13]. A detailed description of our data acquisition and analysis routines was recently published [14]. Here, we present a latitudinal map for the [HDO]/[H_2O] ratio taken on 26 March 2008 (L_s = 50.1°), and a longitudinal map of HDO taken with the slit east-west on Mars centered above the sub-Earth point for 3 April 2010 (L_s = 72.5°).

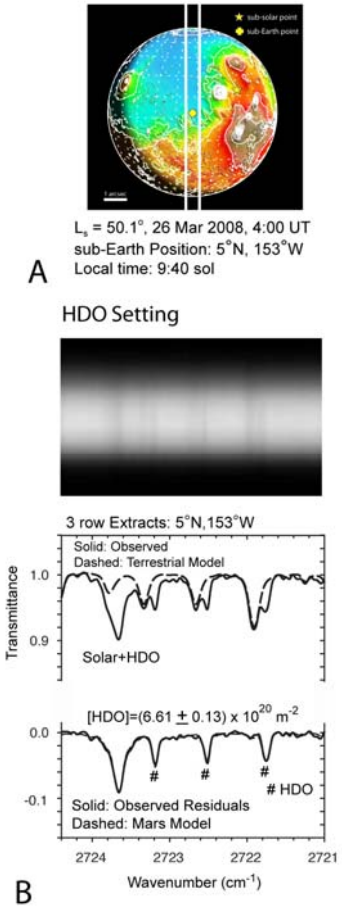

Fig. 1.A. Position of the spectrometer slit on the image of Mars for data taken at L_s = 50.1°. The slit was aligned N-S on Mars and centered on the sub-Earth location (yellow cross); the sub-solar position is indicated by a yellow star. The topographic map was generated using Mars24 [19]. **B.** A spectral/spatial image taken by CSHELL on the NASA-IRTF at an HDO setting. Three row extracts provide the spectrum centered at the sub-Earth latitude. A terrestrial atmospheric model is constructed to fit the observed spectrum (upper trace). The model is subtracted from the observed spectrum (lower trace). The column density of HDO is obtained by constructing Mars atmospheric models to fit the residuals. The equivalent widths of the indicated (#) HDO lines are significantly larger than the retrieved noise level (1-σ) of (0.0001 cm^{-1}) [14].

Observations:

Data were obtained using CSHELL [15] at the NASA-IRTF. The 0.5 x 30 arc-sec slit was positioned north-south (or east-west) on Mars as in Fig. 1A. Spectral/spatial images were obtained by nodding the telescope 15 arc-sec along the slit in an abba sequence. A spectral/spatial image (four-minute integration time on Mars) at an HDO setting (2722.5 cm^{-1}) appears in Fig. 1B. Three row extracts from this image are analyzed using a line by line radiative transfer model (LBLRTM) [16] to obtain the vertical column density of HDO on Mars.

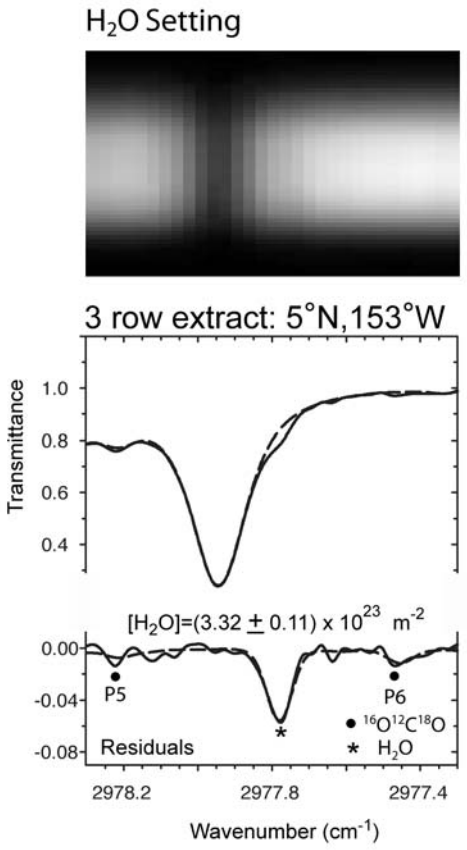

Fig. 2. Spectral/spatial image taken at an H_2O setting. The image clearly shows the absorption in Earth's atmosphere. The upper trace is a three-row extract from the image (solid curve). A terrestrial model (dashed curved) is subtracted from the observed curve to produce the residual plot in the lower trace. A Mars atmospheric model is fitted to the residual to obtain the [H_2O] value. Two absorption lines of an isotopic form of carbon dioxide are indicated. [20]

The column density of H_2O is similarly measured using a different spectral setting (Fig. 2) From the nearly simultaneous spectral/spatial images at HDO and H_2O settings, the [HDO]/[H2O] ratio is determine for an atmospheric location above Mars' surface.

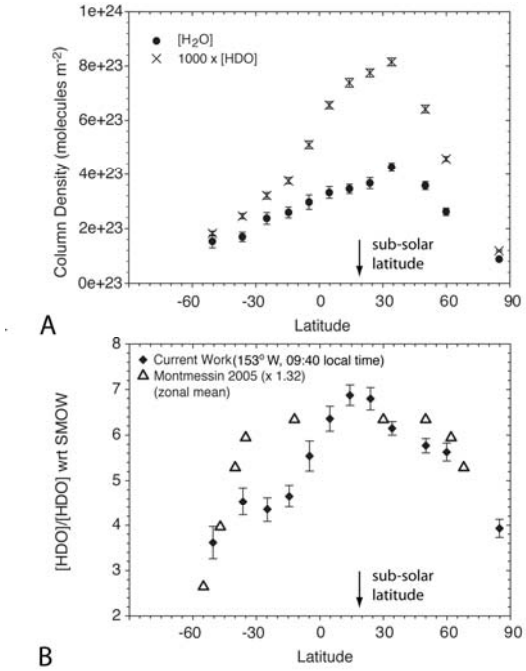

Fig. 3. **A.** Column densities of HDO and H_2O measured with spectral extracts at three row intervals (0.6 arc-sec) for the data taken on 26 Mar 2008. **B.** Ratios between HDO and H_2O compared to their ratio on Earth (VSMOW). Our results for L_s = 50° are presented along with predictions of Montmessin [1] (multiplied by 1.32) for the same season [14].

a. Latitudinal maps for L_s = 50.1°: From data acquired on 26 March 2008, we constructed latitudinal maps centered at 153°W. The acquired column densities appear in Fig. 3A. Their measured ratios (relative to Vienna Standard Mean Ocean Water, VSMOW, [HDO]/[H2O] = 3.1 x 10^{-4}) are given in Fig. 3B. Our results indicate that the mean ratio differs greatly from that of the Earth and that the specific ratio depends on latitude (and possibly season). The ratio peaks near the sub-solar latitude and decreases towards both poles. The values predicted by the model of Montmessin [1] for L_s = 50° are multiplied by a factor (1.32) so that the mean values in the sub-solar region match our measured values. Montmessin uses a ratio of 5.6 for [HDO]/[H2O] in the north polar cap but suggests that 6.5 might be closer to the true value – our results suggest that this is so. Atmospheric temperatures decrease from the sub-solar latitude to the poles causing a general decrease in water vapor abundance; however, ice aerosols could become enriched in deuterium owing to preferential condensation of HDO molecules (Vapor Pressure Isotope Effect) – similar to the enrichment of raindrops on Earth. Our measurements of the [HDO]/[H2O] vapor phase abundance ratio indicate a strong gradient with latitude – both the latitudinal and the quantitative values agree with the pattern predicted by the longitudinally averaged Montmessin model[1].

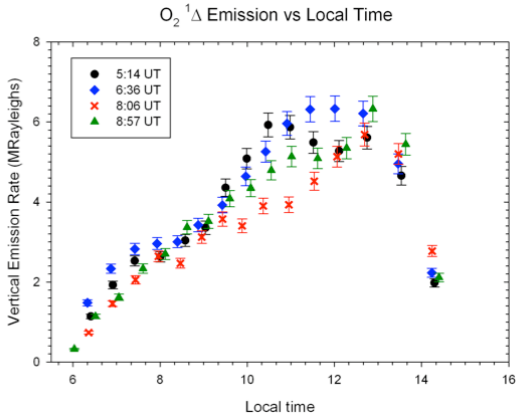

Fig. 4. Results of the $O_2(^1\Delta)$ emission measurements of 3 Apr 2010 adjusted for local time. These taken over a 3.5 hour time interval and are shown to peak near 12:00 LT independent of local geography.

b. Diurnal maps for L_s = 72.5°: From data taken at L_s = 50.1°, Villanueva [12] produced global maps that also show strong variations with longitude and local time. Those maps were produce with the spectrometer slit north-south on Mars and stepped at 1.0 arc-sec intervals east-west.

To test the longitudinal and diurnal variation, we positioned the slit east-west on Mars on 3 April 2010 (L_s = 72.5°). The slit was centered on the sub-Earth point (14.2°N) for four hours while data were repeatedly taken at HDO, H_2O, and $O_2(^1\Delta)$ emission settings. Twelve sets of data for each of these spectral settings were acquired. Preliminary reductions indicate that the $O_2(^1\Delta)$ emissions do not vary with local geography (surface altitude), but increase between sunrise and 12:00 local time (Fig. 4). The intensity decreases afterwards. The presence of these emissions at low latitudes also suggests that the hygropause is located at altitudes of less than 15 km. The rotational temperature of the $O_2(^1\Delta)$ emissions indicates an altitude above 25 km [17].

Results for the HDO column densities over a 3.5 hour period time appear in Fig. 5A. For the region east of Syrtis Major, [HDO] is constant. The column density is larger over Syrtis Major and further increases over Arabia Terra as it emerges from the Mars night. In Fig. 5B, values for 275°W and 340°W are plotted with respect to local time. Values for [HDO] near 275°W are constant between 9:30 and 13:00 LT, but near 340°W, [HDO] increases considerably between 6:50 and 9:00 LT. This latter region contains sub-surface hydrogen and is a location where methane has been found [2]. The reason for the increase in [HDO] after sunrise could possibly be the sublimation of ground-frost or water-ice clouds accumulated during the night, or a release from the sub-surface. It merits further study.

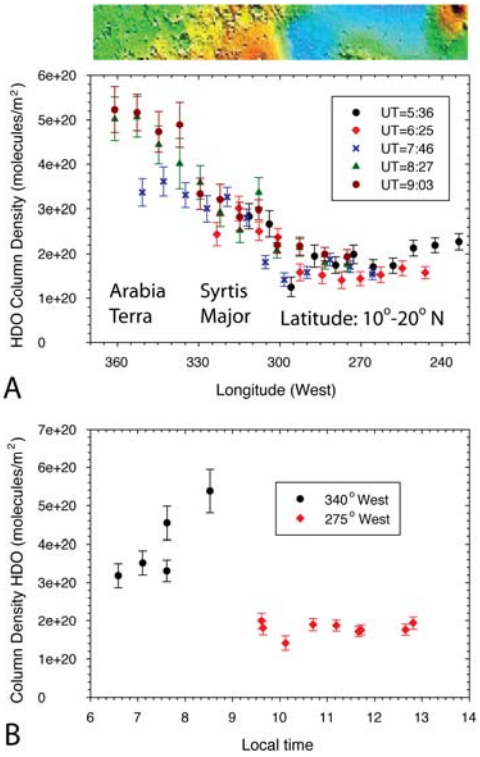

Fig. 5. On 3 Apr 2010 (L_s = 72.5°), the slit was placed east-west across Mars centered at the sub-Earth latitude (14.2° N). The sub-Solar latitude was 24.2° N. Spectral/spatial images (4 minutes integration time) at an HDO were taken over a four-hour period. **A.** Measured column densities of HDO taken at five times during this period. The cropped Mars-MOLA map indicates the location of the retrieved points. **B.** Retrieved data points centered at 275° and 340° adjusted to local time.

Data at the H_2O setting are currently being processed. The diurnal variation of the D/H ratio could provide insights into the source of water vapor in the atmosphere.

Conclusion and Future Plans:

We present a latitudinal map of the [HDO]/[H_2O] ratio for L_s = 50.1° that peaks near the sub-solar latitude and is consistent with the longitudinally averaged model of Montmessin [1]. For L_s = 72.5°, we show a longitudinal map (centered at 14°N) for [HDO] taken over a four-hour period between 230° and 360°W. [HDO] is constant at 275°W over the four hours but increases at 340°W during the three hours after sunrise. Using updated analysis tools [14] we intend to further analyze recent data and reanalyze previously taken data from 2003-2008. We plan to obtain data during the upcoming Mars apparitions and to use ISHELL [18] which is currently

being constructed at the NASA-IRTF. ISHELL is a cross-dispersed IR-spectrograph that can measure both HDO and H_2O bands simultaneously with better sensitivity than CSHELL.

Acknowledgements:

REN was supported by NSF RUI Grant AST-0805540. MJM and GLV were supported by Grants from NASA's Planetary Astronomy Program (344-32-51-96) and Astrobiology Program (344-53-51). We acknowledge the Director and Staff of the NASA Infrared Telescope Facility for granting us observing time. The NASA-IRTF is operated by the University of Hawaii under Cooperative Agreement NNX-08AE38A with the National Aeronautics and Space Administration, Science Mission Directorate, Planetary Astronomy Program.

References:

[1] Montmessin F. et al. (2005), *J. Geophys. Res.*, **110**, E03006. [2] Mumma M.J. et al., (2009), *Science*, **323**, 1041-1045. [3] Formisano V. et al, (2004), *Science*, **306**, 1758-1761. [4] Kranopolsky V. et al., (2004), *Icarus*, **172**, 537-547. [5] Atreya, S. et al., (2007) *Planet. Space Sci*., **55**, 358-369. [6] Lefevre F. and Forget, F., (2009), *Nature*, **460**, 720-723. [7] DiSanti, M. and Mumma, M (1995), *Workshop on Mars Telescope Observations*, (Cornell U. Press). [8] Novak, R. et al., (2002), *Icarus*, **158**, 14-23. [9] Smith, M., (2007), *Icarus*, **167**, 148-165. [10] Mumma, M. et al. (2003), Sixth International Conference on Mars, Abstract # 3186. [11] Novak R. et al. (2007), Seventh International Conference on Mars, Abstract # 3283. [12] Villanueva et al., (2008) Mars Atmosphere: Modelling and Observations, Abstract # 9101. [13] Fisher, D. et al. (2008), *J. Geophys. Res.*, **113**, E00A15. [14] Novak R. et al. (2010a), *Planet. Space Sci*., doi:10.1016/j.pss.2010.06.017. [15] Greene et al., (1993), *Proc. SPIE*, **1946**, 313-324. [16] Clough S., et al (2005), *JQSRT*, **91**, 233-244. [17] Novak et al. (2010b), *B.A.A.S*, **42**, 1041. [18] Tokunaga et al, (2008), *Proc. SPIE*, **7014**, 70146A-70146A-11. [19] Schmunk R and Allison, M. (2008), <www.giss.nasa.gov/tools/Mars24>. [20] Villanueva G.L. et al., (2008), *Icarus*, **195**, 34-44.